Does pulsed field ablation regress over time? A quantitative temporal analysis of pulmonary vein isolation ⓔ

Iwanari Kawamura, MD,* Petr Neuzil, MD, PhD,† Poojita Shrivamurthy, MD,*
Jan Petru, MD,† Moritoshi Funasako, MD, PhD,† Kentaro Minami, MD,†
Kenji Kuroki, MD, PhD,* Srinivas R. Dukkipati, MD,* Jacob S. Koruth, MD,*
Vivek Y. Reddy, MD*†

From the *Department of Cardiology, Helmsley Electrophysiology Center, Icahn School of Medicine at
Mount Sinai, New York, New York, and †Department of Cardiology, Homolka Hospital, Prague, Czech
Republic.

BACKGROUND The tissue specificity of pulsed field ablation (PFA) makes it an attractive energy source for pulmonary vein (PV) isolation (PVI). However, beyond each PFA lesion's zone of irreversible electroporation and cell death, there may be a surrounding zone of reversible electroporation and cell injury that could potentially normalize with time.

OBJECTIVE The purpose of this study was to assess whether the level of electrical PVI that is observed acutely after PFA regresses over time.

METHODS In a clinical trial, patients with paroxysmal atrial fibrillation underwent PVI using a biphasic PFA waveform delivered through a dedicated, variably deployable multielectrode basket/ flower catheter. Detailed voltage maps were created using a multispline diagnostic catheter immediately after PFA and again ~3 months later in a prospective, protocol-specified reassessment procedure. We analyzed 20 patients who underwent PFA with durable PVI and available maps from both time points. To compare the ablated zones, the left- and right-sided PV antral isolation areas and

nonablated posterior wall area were quantified and the distances between left and right PV low-voltage edges were measured.

RESULTS A comparison of voltage maps immediately after PFA and at a median of 84 days (interquartile range 69–90 days) later revealed that there was no significant difference in either the left- and right-sided PV antral isolation areas or nonablated posterior wall area. The distances between low-voltage edges on the posterior wall were also not significantly different between the 2 time points.

CONCLUSION This study demonstrates that the level of PV antral isolation after PFA with a multielectrode PFA catheter persists without regression.

KEYWORDS Atrial fibrillation; Electroporation; Level of isolation; Pulmonary vein isolation; Pulsed field ablation

(Heart Rhythm 2021;■:1–7) © 2021 Heart Rhythm Society. This is an open access article under the CC BY-NC-ND license (http://creativecommons.org/licenses/by-nc-nd/4.0/).

Introduction

Pulsed field ablation (PFA) is a nonthermal energy modality that is unique in having tissue-selective ablative properties.[1–7] Using a custom PFA generator able to deliver a custom hierarchical pulse sequence, a dedicated PFA catheter was shown to be safe and effective in electrically isolating *porcine* thoracic vessels—pulmonary veins (PVs) and superior vena cava. Histological analysis demonstrated

similar transmurality to radiofrequency ablation, but without the attendant collateral injury.[8] Furthermore, clinical experience with the system demonstrated that PFA results in acute safety and feasibility as well as durable PV isolation (PVI).[9]

While the goal of PFA is irreversible injury to ensure lesion chronicity, depending on the device design and pulse parameters used by a given system, cell permeabilization

with PFA also has the potential to be reversible. That is, cells may survive because of the reestablishment of cell membrane integrity and electrical homeostasis.[10] Thus, beyond each PFA lesion's zone of *irreversible* electroporation and cell death, there may be a surrounding zone of *reversible* electroporation with acute cell injury that recovers with time.

In patients, while we have previously demonstrated that electrical PVI with PFA is largely durable,[9] this durability does not necessarily mean that the *level* of electrical isolation does not regress. That is, PVs may remain isolated, but the level of isolation may be more ostial than an initial antral lesion set. Indeed, when the chronic level of PVI after cryoballoon ablation was evaluated, the level of isolation was not as proximal/antral as previously reported for acute cryoballoon ablation, suggesting that the level of isolation regresses over time.[11] Accordingly, we performed this analysis to determine whether the *level of electrical PVI* that is observed acutely after PFA regresses over time in the patient with durable PVI.

Methods
Data source
The present study is retrospective and uses clinical data from PEFCAT (A Safety and Feasibility Study of the FARAPULSE Endocardial Ablation System to Treat Paroxysmal Atrial Fibrillation; ClinicalTrials.gov identifier NCT03714178)—a single-arm feasibility study of PFA conducted at Homolka Hospital, Prague, and the Centre Hospitalier Universitaire de Bordeaux, Bordeaux, France. The population analyzed herein was exclusively derived from the former institution. The study sponsor, Farapulse of Menlo Park, CA, is the manufacturer of the PFA system. The research reported in this article adhered to Helsinki Declaration as revised in 2013, and ethics committee approval had been obtained.

Study population
At the time of analysis, Homolka Hospital had enrolled 50 patients with symptomatic paroxysmal atrial fibrillation resistant to antiarrhythmic medications in PEFCAT. Included patients were required to have a left ventricular ejection fraction of >40% and a left atrial (LA) anteroposterior dimension of <5.0 cm. There were no exclusions for PV anatomy. Of these patients, 45 underwent invasive PV reassessment. This retrospective analysis included all patients who had (1) durable PVI upon invasive reassessment, (2) available electroanatomic maps from both the baseline and reassessment time points, and (3) voltage maps created by the same electroanatomic mapping system at both time points.

Index and reassessment procedures
Patients underwent preprocedural computed tomography scanning to characterize PV anatomy. After informed consent, the LA appendage was assessed for thrombus by intracardiac echocardiography (AcuNav, Siemens, Munich, Germany). Oral anticoagulation was uninterrupted, and intravenous heparin was administered before transseptal puncture. As per the PEFCAT protocol, a biphasic waveform was used during the trial as previously described.[9]

After femoral venous access, a 12-F over-the-wire PFA catheter (Farapulse) was advanced through a 13-F deflectable sheath to the LA via transseptal puncture. The PVI workflow was performed under moderate sedation with fentanyl, benzodiazepines, and propofol. The study catheter had 5 splines, each with 4 electrodes, and could be variably deployed between a flat "flower" and a more spherical "basket" configuration to suit individual PV anatomy. In the study procedures, the catheter was advanced over a guidewire such that the splines achieved circumferential contact/proximity with the PV antra (Figure 1). The catheter was rotated between applications to ensure circumferential PV ostial and antral coverage. At the beginning of the study, a standard electrophysiology catheter paced the ventricles during ablation to synchronize the pulses to just after QRS onset; however, this practice was later abandoned to optimize workflow. The therapeutic waveform is structured as a hierarchical set of microsecond-scale pulses emitted in a bipolar fashion between the electrodes. The generator output ranged from 1800 to 2000 V per application. After ablation, a circular mapping catheter (Lasso, Biosense Webster, Irvine, CA) assessed electrical PV activity and postablation voltage mapping was performed using a multielectrode mapping catheter (PentaRay, Biosense Webster). At the investigator's discretion, adenosine boluses (12–18 mg each) were administered to identify dormant PV conduction.

Patients underwent invasive reassessment electrophysiological mapping at 75 days after the index ablation procedure. During this repeat procedure, the durability of PVI was assessed using a multielectrode catheter; an electroanatomic voltage amplitude map was again created.

Voltage mapping and measurements
The 3-dimensional geometry of the LA and PVs was reconstructed, and high-density bipolar voltage mapping was performed using an electroanatomic mapping system and multispline mapping catheter (CARTO3 and PentaRay, Biosense Webster) at both the aforementioned time points. For the purpose of comparison, *peak-to-peak bipolar electrogram amplitude < 0.5 mV* was defined as the low-voltage threshold for all maps in accordance with previous studies.[12–14]

The PV ostium was identified by 2 electrophysiologists as the point of maximal inflection between the PV wall and the LA wall, and the *PV antrum* was defined as the region proximal to the PV ostium excluding the PVs. In patients with a common PV, we defined the *second branch of common trunk* as PV ostium.[15] The *LA posterior wall surface area* was defined as the area bordered by PV lesions and 2 lines connecting the most superior-and inferior-most aspects of the circumferential ablation lines, respectively.

The surface areas of the isolated left- and right-sided PV antra and nonablated posterior wall were quantified.
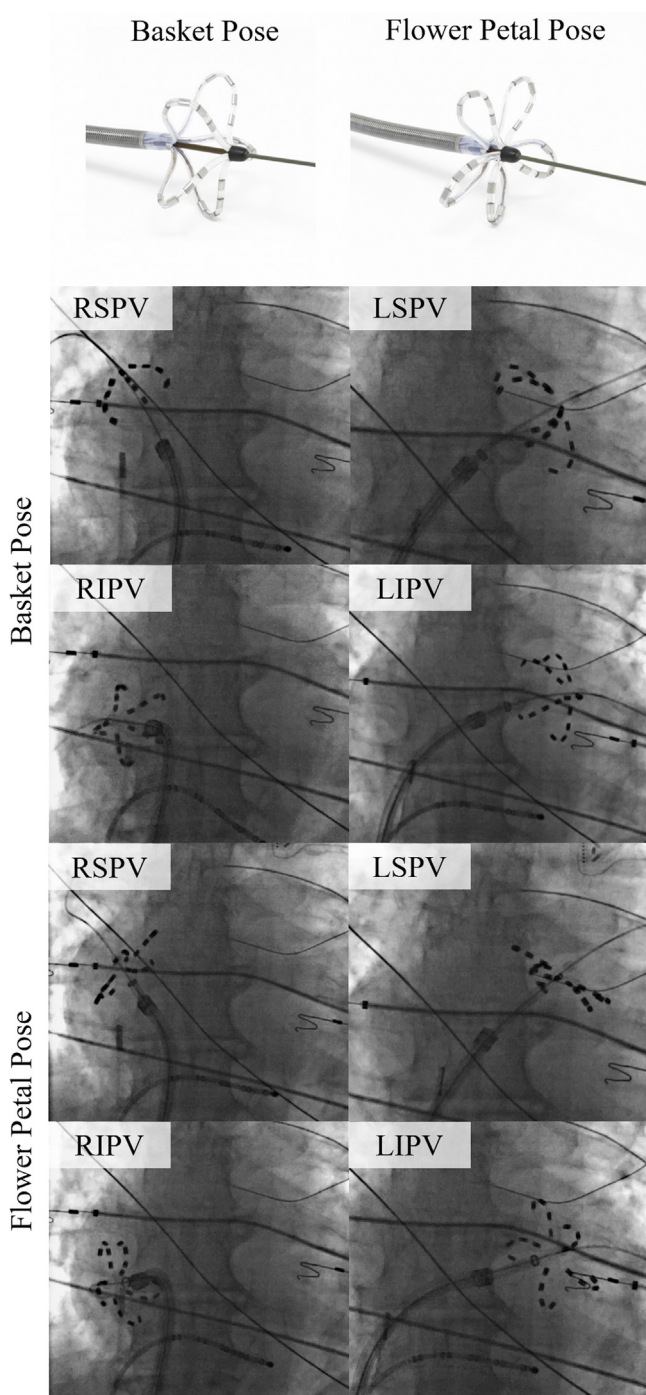
Figure 1 Fluoroscopic imaging during pulsed field ablation. The pulsed field ablation catheter (shown in both flower and basket poses) is positioned at the ostia of various pulmonary veins. LIPV = left inferior pulmonary vein; LSPV = left superior pulmonary vein; RIPV = right inferior pulmonary vein; RSPV = right superior pulmonary vein.

Additionally, the distances between left and right PV low-voltage borders were measured on voltage maps created immediately after PFA, during the index ablation procedure, as well as during invasive reassessment ∼3 months later to characterize lesion regression (Figure 2). The CARTO system automatically calculated the surface area and the distance from manually selected points. Each pair of voltage maps

was registered to the patient 3-dimensional computed tomography models to improve accuracy.

Statistical analysis

Data were tested using the Kolmogorov-Smirnov test and are presented as mean ± SD for normally distributed variables. Median and interquartile range (IQR) are given for nonnormally distributed variables. Values of categorical variables were reported as number and percentage of patients. Continuous variables were compared between the groups by using the Wilcoxon rank sum test or Student t test, as appropriate. A P value of <.05 was considered significant. All analyses were performed using SPSS version 24.0 (IBM Corporation, Armonk, NY).

Results

Patient characteristics and procedure characteristics

Of the 45 patients at our center who underwent remapping procedures, 38 (84%) fulfilled the criterion of all PVs with durable isolation. Among the durably isolated patient cohort, 18 (of 38) patients were subsequently excluded because of the lack of available voltage maps at the time of reassessment (eg, durable isolation confirmed without mapping) or because of incongruent mapping systems/catheters used at the 2 time points. A total of 20 patients fulfilled all our 3 inclusion criteria and were analyzed herein. They were relatively young (56.0 ± 11.6 years), male predominant (75%), with preserved left ventricular function (63.6% ± 3.7%), and mild LA enlargement (41.7 ± 5.0 mm) (Table 1). Two patients had left common PVs.

A modern biphasic waveform was used in all patients, resulting in all procedures being performed with moderate sedation and without paralytic agents. The majority of patients (80%; 16 of 20 patients) were treated with an optimized delivery protocol, previously referred to as the biphasic-3 waveform.[9] The mean fluoroscopy time was 9.1 ± 3.0 minutes. The *total procedure time*, defined as the time from femoral access to closure, was 81.0 ± 20.0 minutes. PVI was achieved in 100% of PVs (78 of 78), and there were no acute reconnections during a postablation waiting period (voltage mapping) or upon provocative adenosine testing, when performed (n = 3 patients). There were no clinical instances of PV stenosis, stroke or transient ischemic attack, phrenic nerve injury, or atrioesophageal fistula. PV reassessment procedures confirmed lesion durability and occurred at a median of 84 days (IQR 69–90 days) without complications.

Mapping data and quantitative analysis

The number of electrogram points acquired during electroanatomic mapping was 653 (IQR 571–736) and 874 (IQR 520–1228) in the index and invasive reassessment procedures (P = .876). One patient presented with atypical atrial flutter during mapping in the chronic phase (patient 12); otherwise, all patients were in sinus rhythm.
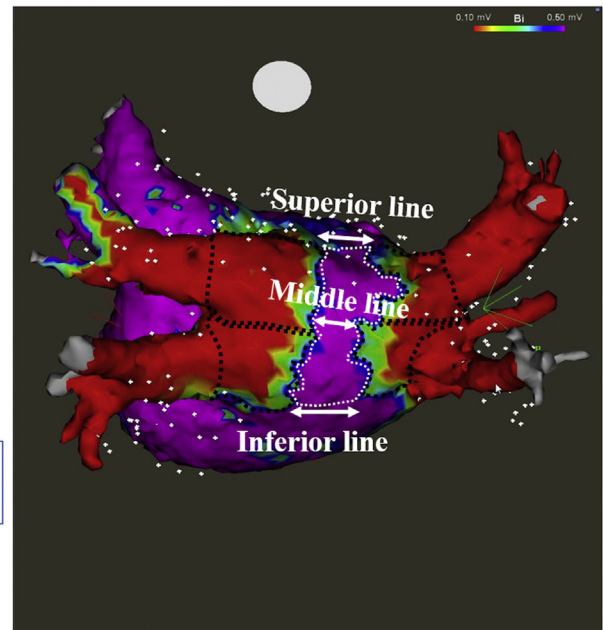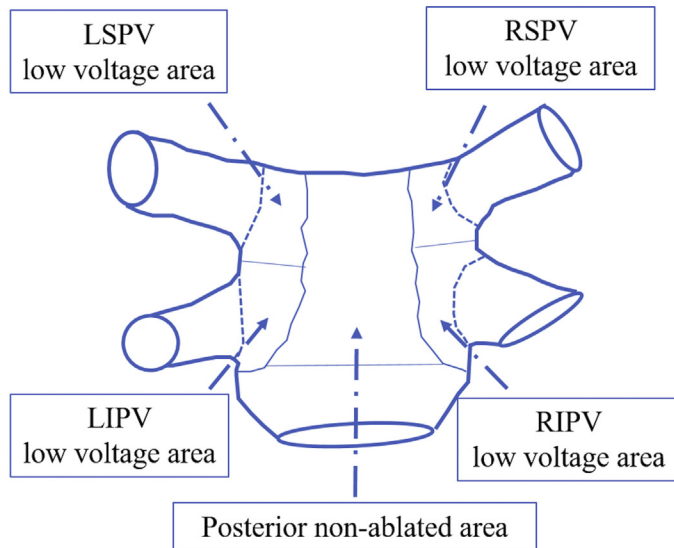
Figure 2 Methodology for measurements of area and distances. The surfaces of the left- and right-sided pulmonary vein antral isolation areas and nonablated posterior wall area were quantified. The distances between left and right pulmonary vein low-voltage edges were measured on voltage maps created immediately after pulsed field ablation and during invasive reassessment to characterize lesion regression. LIPV = left inferior pulmonary vein; LSPV = left superior pulmonary vein; RIPV = right inferior pulmonary vein; RSPV = right superior pulmonary vein.

During the index procedure, the electrical isolation areas of the antra of the left PV and right PV were 6.40 ± 2.32 and 5.03 ± 2.12 cm², respectively. The mean surface area of the nonablated posterior wall was 10.73 ± 4.01 cm². In total, 48.0% ± 11.0% of the posterior LA wall remained electrically intact and unablated.

The isolated areas of each of the 4 PV antra were not significantly different between the 2 time points (left superior PV: 3.30 ± 1.43 cm² vs 3.35 ± 1.58 cm², P = .739; left inferior PV: 3.10 ± 1.14 cm² vs 2.76 ± 1.24 cm², P = .239; right superior PV: 2.64 ± 1.30 cm² vs 2.44 ± 0.86 cm², P = .358; and right inferior PV: 2.43 ± 1.15 cm² vs

Table 1 Patient characteristics (N = 20)

Characteristic	Value
Age (y)	56.0 ± 11.6
Male sex	15 (75.0)
LA diameter (mm)	41.7 ± 5.0
LVEF (%)	63.6 ± 3.7
Hypertension	13 (65.0)
Diabetes	2 (10.0)
Stroke or TIA	1 (5.0)
CAD (MI/CABG)	0 (0.0)
Anticoagulation	
Warfarin	7 (35.0)
NOAC	9 (45.0)
None	4 (20.0)
Antiarrhythmic drugs	
Class I	11 (55.0)
Class II	18 (90.0)
Class III	0 (0.0)
None	1 (5.0)
Left common PV	2 (10.0)
Procedure details	
Fluoroscopy time (min)	9.1 ± 3.0
Procedure time (min)	81.0 ± 20.0
Follow-up date (d)	84 (69–90)

Values are presented as mean ± SD, median (interquartile range), or n (%).

CABG = coronary artery bypass grafting; CAD = coronary artery disease; LA = left atrial; LVEF = left ventricular ejection fraction; NOAC = novel oral anticoagulant; MI = myocardial infarction; PV = pulmonary vein; TIA = transient ischemic attack.

Table 2 Comparison of isolation line between acute and follow-up

Variable	Acute (n = 20)	Follow-up (n = 20)	P
LPV total (cm²)	6.40 ± 2.32	6.22 ± 2.69	.589
LSPV (cm²)	3.30 ± 1.43	3.35 ± 1.58	.739
LIPV (cm²)	3.10 ± 1.14	2.76 ± 1.24	.239
RPV total (cm²)	5.03 ± 2.12	4.73 ± 1.49	.372
RSPV (cm²)	2.64 ± 1.30	2.44 ± 0.86	.358
RIPV (cm²)	2.39 ± 1.15	2.29 ± 0.90	.604
PV total (cm²)	11.43 ± 3.69	10.95 ± 3.41	.114
Superior line (mm)	24.23 ± 7.13	25.60 ± 9.59	.320
Middle line (mm)	25.52 ± 7.88	26.23 ± 7.94	.667
Inferior line (mm)	29.19 ± 9.36	30.57 ± 9.06	.304
Nonablated area (cm²)	10.73 ± 4.01	10.74 ± 3.66	.974
Nonablated area/total LAPW (%)	48.0 ± 11.0	49.2 ± 10.0	.329
Number of points	653 (571–736)	874 (520–1228)	.876

Values are presented as mean ± SD or median (interquartile range).

LAPW = left atrial posterior wall; LIPV = left inferior pulmonary vein; LPV = left pulmonary vein; LSPV = left superior pulmonary vein; PV = pulmonary vein; RIPV = right inferior pulmonary vein; RPV = right pulmonary vein; RSPV = right superior pulmonary vein.
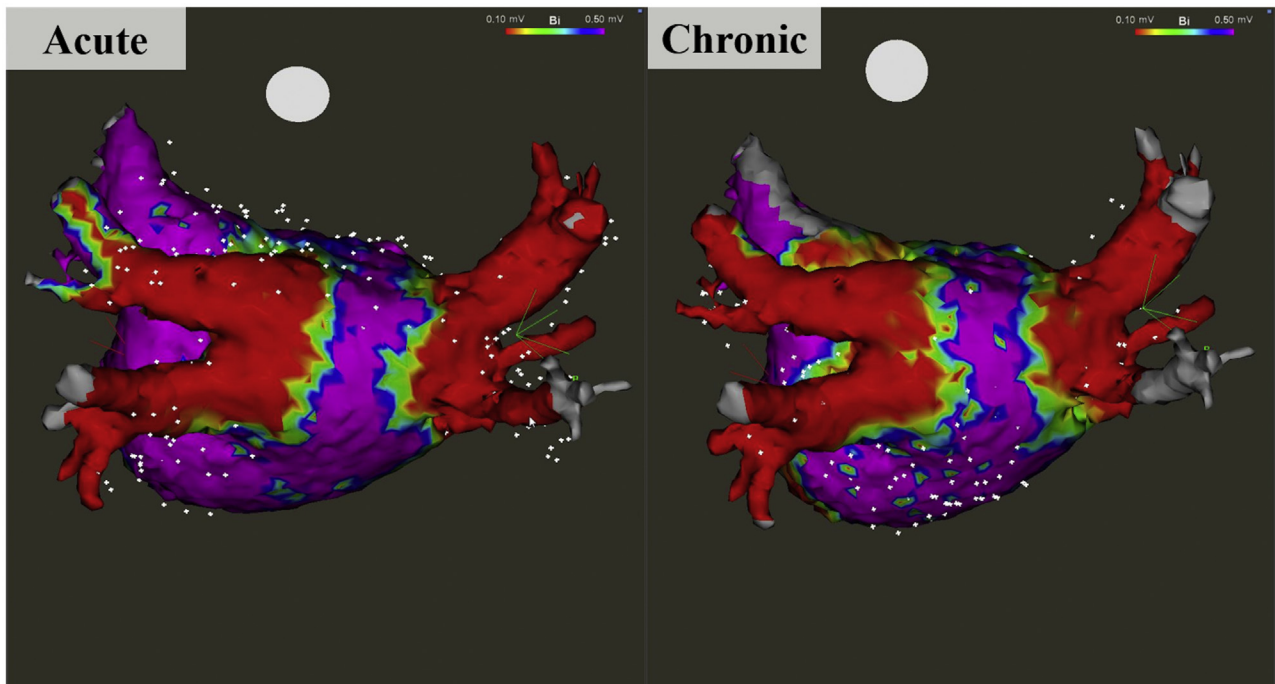
Figure 3   Voltage maps from acute and chronic phases. The isolated areas of each of the 4 pulmonary vein antra persisted without significant regression over time.

2.25 $\pm$ 0.89 cm^2, P = .604) (Table 2 and Figure 3). The pairs of voltage maps for each patient are shown in Online Supplemental Figure 1, and the ratio of the Δ isolated area to the index isolated area is described in Figure 4. Two patients (patients 1 and 15) and 1 patient (patient 3) had >20% regression and progression, respectively (Online Supplemental Figure 2). The nonablated area on the posterior wall (10.74 $\pm$ 4.01 cm^2 vs 10.73 $\pm$ 3.66 cm^2; P = .974) and the ratio of the intact posterior LA area to the total posterior LA (48.0 $\pm$ 11.0 vs 49.2 $\pm$ 10.0; P = .329) were also similar between the 2 time points. The distances between low-voltage edges on the posterior wall were also not significantly different between the 2 time points (Table 2 and Figure 3).

Discussion

To our knowledge, this is the first study to quantitatively assess whether the level of electrical PVI that is observed acutely after PFA regresses over time. In this study of PVI in patients with paroxysmal AF using a multielectrode basket/flower PFA catheter, invasive electroanatomic mapping $\sim$3 months after the index ablation procedure demonstrated a preserved level of electrical PVI without regression.

The possibility of lesion regression after electroporation

Electroporation is best described by the theory of aqueous pore formation. According to this theory, the electric field induces a voltage across the bilayer and reduces the energy required for spontaneous formation of aqueous pores in the bilayer, thus facilitating the formation of a higher number

of pores, and pores that are more stable, than in the absence of the electric field. Forming and stabilizing under the influence of the electric field, pores have lifetimes ranging from milliseconds up to minutes after the field is removed. Because pores then reseal, they are categorized as metastable. Depending on the electric pulse delivery settings, permeabilization of cells can be reversible, meaning the cell can survive because of the reestablishment of cell membrane integrity and electrical homeostasis.[3] Indeed, reversible electroporation is commonly purposely used for cellular gene transfection since the early 1980s.[16] Reversible electroporation has important applications in tissue as a method for gene insertion in cells (electrogenetherapy) and for the introduction of potent but normally impermeable anticancer drugs such as bleomycin (electrochemotherapy).[17] Accordingly, we hypothesized that beyond each PFA lesion's zone of irreversible electroporation and cell death, there may be a penumbra of reversible electroporation and cell injury that normalizes with time.

Isolation area after PFA

Since excessive thermal ablation within the PVs causes vein stenosis, an extraostial ablation strategy targeting the PV antra has been widely used. Of the various catheter ablation techniques available, PV antrum isolation is also thought to result in better rhythm outcome than segmental PVI for patients with paroxysmal AF. In 1 study, a larger PV antrum isolation area resulted in better freedom from AF and macro-reentrant tachycardia.[15] Another study demonstrated that non-PV foci were situated at the left superior PV antrum, just outside the isolation zone created by cryoballoon ablation, but inside the wide circumferential PVI line.[11]
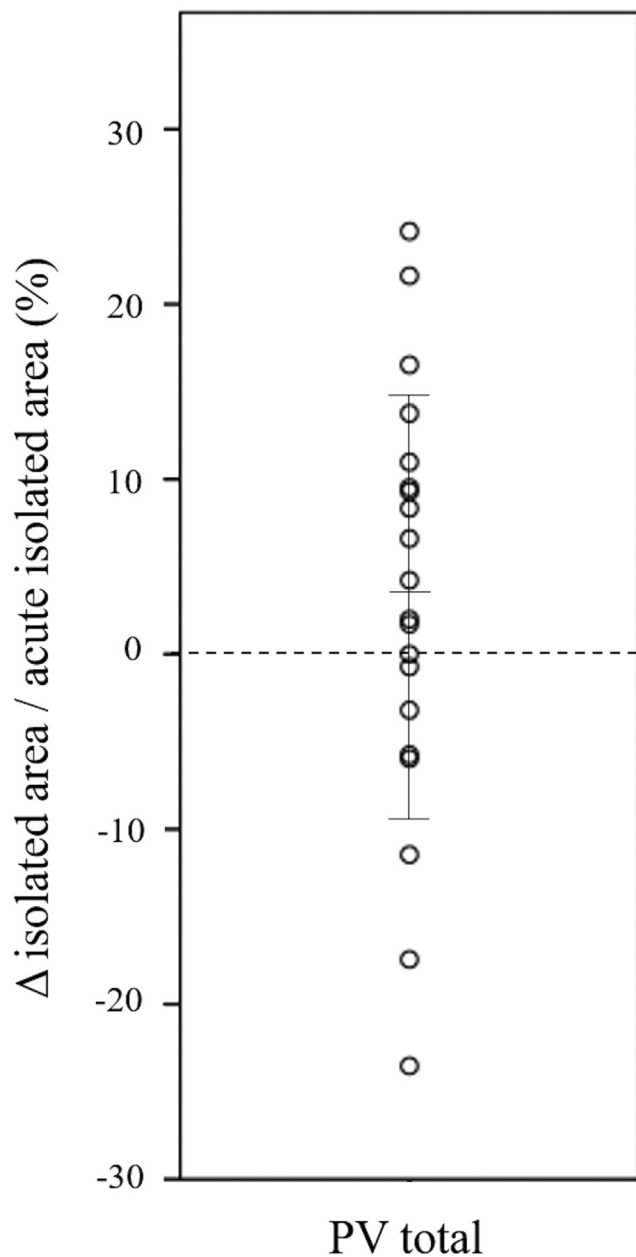
Figure 4 Distribution of the ratio of the Δ isolated area to the acute isolated area. Δ isolated areas were calculated by subtracting the chronic and acute isolated areas. Two patients and 1 patient had >20% regression and progression, respectively. PV = pulmonary vein.

Accordingly, there has been a general desire to ensure that PVI lesion sets isolate proximally to encompass the PV antral regions.

By using an ablative electric field, PFA does not require full contact on the tissue—though tissue proximity is necessary. Although rapid, safe, durable PVI has been demonstrated using the multielectrode PFA catheter, we did not have a quantitative understanding of the location of the PVI line. For example, the isolation areas of both PVs and the nonisolated posterior wall after cryoballoon PVI were recently quantified: left PV isolation area, right PV isolation area, and nonisolation areas were 4.6 ± 1.9, 4.8 ± 2.6, and

16.1 ± 5.5 cm^2, respectively.[18] But since the scar criteria were set at <0.1 mV, it is difficult to compare these data directly with our study. Interestingly, another study reported nearly the same nonablated posterior area as observed in our cohort (8.4–17.0 cm^2).[11,19]

Temporal effect of the level of PVI
Several studies have evaluated the electrical isolation area after thermal ablation with various energy sources—focal radiofrequency ablation, cryoballoon, laser balloon, or hot balloon.[15,19–21] However, little has been published regarding any change in the isolation zone by comparing between 2 time points.

One study investigated the chronic isolation area in 32 patients who underwent cryoballoon ablation, followed by a repeat procedure to assess for chronic regression in 17 patients with, and 15 without, arrhythmia recurrence.[11] Interestingly, the area of LA posterior wall isolation appeared regressed relative to the acute postablation level expected after cryoballoon ablation. It was hypothesized that edematous tissue bordering the acute cryolesions might contribute to the low-voltage area in the index map, increasing the apparent lesion size at that initial time point.

In contrast, using the same PFA system as used in our study, we observed in preclinical *porcine* experiments that PFA lesions were composed of the organized homogeneous fibrotic replacement of the myocardium and contained fewer signatures of inflammatory response than did radiofrequency ablation lesions.[8] Such robust PFA lesion characteristics would support the lack of substantial regression in the PVI level of isolation in our study. Indeed, the nonablated area on the posterior wall, expressed as the ratio of the intact posterior LA area to the total posterior LA, was similar in the acute (48%) and chronic (49%) phases post-PFA observed in our study to that reported in the chronic (48%) phase post–cryoballoon ablation.[11]

It should be appreciated that there is some controversy regarding the voltage amplitude cutoff to define scar. In a recent study, *low voltage* was defined as <0.5 mV on high resolution electroanatomic mapping in the chronic phase, as confirmed by high output pacing[11]; this cutoff was also used acutely in other studies.[12–14] Accordingly, we used this approach in our analyses. However, in 1 set of studies, different thresholds were evaluated to define scar (using absence of pace capture as the criterion standard), both in acute postablation setting and during chronic redo procedures.[22,23] These studies identified the ideal acute and chronic scar ranges to be 0.2–0.45 and 0.15–0.20 mV, respectively. When we compared our standard cutoffs with these cutoffs, the acute isolation areas were not substantially different, but the chronic isolation areas were slightly decreased by using these revised criteria (see Online Supplemental Figure 3).

Study limitations
This study was retrospective on the basis of the secondary use of data from PEFCAT, and the sample size was relatively

small. Only patients with paroxysmal AF were studied. The outcomes were all derived from a single center, since the second site in the PFA trials was excluded either because mapping had not been performed in the remapping procedure or because of the use of incongruent mapping systems/catheters. To minimize the chance for bias, we also assessed PV durability at this second site—91.8% PVI durability when the optimized waveform (biphasic-3 waveform) was used (56 of 61 PVs).

The chronic assessments were conducted ∼3 months after index PFA, and one cannot rule out the possibility of regression at very late time points post-PFA; however, preclinical histology data suggest that additional inflammatory changes or lesion remodeling is unlikely beyond this time point.[8] The relative level of PVI between PFA and thermal ablation is not known from the results of this study; this must be analyzed directly in patients undergoing ablation with these various energy sources—ideally in a randomized study, but at least using identical measurement methodology.

This study includes quantitative assessment from only the posterior LA because, from a technical standpoint, measuring the anterior level of isolation for left PVs is difficult to calculate in some patients with the tools currently available on the electroanatomic mapping system; however, previous studies have similarly focused on the posterior LA isolation area.

Finally, the durability of the extent of PVI observed herein may be predicated on the strategy of bonus applications used. That is, for each PV, PFA applications were delivered in *both* flower and basket poses and included catheter rotation between pairs of applications in the same pose. It is possible that an abbreviated energy delivery strategy might result in less lesion "consolidation," thereby affecting not only the durability of PVI but also the durability of the *extent* of PVI.

Conclusion

This study demonstrates that the level of PV antral isolation after PFA with the multielectrode basket/flower PFA catheter persists without lesion regression upon invasive chronic reassessment. Thus, ablation with this pulsed field system results in a durably nonregressive level of electrical PVI.

Appendix
Supplementary data

Supplementary data associated with this article can be found in the online version at https://doi.org/10.1016/j.hrthm.2021.02.020.

References

1. Davalos RV, Mir LM, Rubinsky B. Tissue ablation with irreversible electroporation. Ann Biomed Eng 2005;33:223–231.
2. Rubinsky B, Onik G, Mikus P. Irreversible electroporation: a new ablation modality—clinical implications. Technol Cancer Res Treat 2007;6:37–48.
3. Kotnik T, Kramar P, Pucihar G, Miklavčič D, Tarek M. Cell membrane electroporation—Part 1: the phenomenon. IEEE Electr Insul Mag 2012;28:14–23.
4. Reddy VY, Koruth J, Jais P, et al. Ablation of atrial fibrillation with pulsed electric fields: an ultra-rapid, tissue-selective modality for cardiac ablation. JACC Clin Electrophysiol 2018;4:987–995.
5. Koruth JS, Kuroki K, Iwasawa J, et al. Endocardial ventricular pulsed field ablation: a proof-of-concept preclinical evaluation. Europace 2020;22:434–439.
6. Koruth J, Kuroki K, Kawamura I, et al. Focal pulsed field ablation for pulmonary vein isolation and linear atrial lesions: a preclinical assessment of safety and durability. Circ Arrhythm Electrophysiol 2020;13:e008716.
7. Kuroki K, Whang W, Eggert C, et al. Ostial dimensional changes after pulmonary vein isolation: pulsed field ablation vs radiofrequency ablation. Heart Rhythm 2020;17:1528–1535.
8. Koruth J, Kuroki K, Iwasawa J, et al. Preclinical evaluation of pulsed field ablation: electrophysiological and histological assessment of thoracic vein isolation. Circ Arrhythm Electrophysiol 2019;12:e007781.
9. Reddy VY, Neuzil P, Koruth JS, et al. Pulsed field ablation for pulmonary vein isolation in atrial fibrillation. J Am Coll Cardiol 2019;74:315–326.
10. Miklavčič D, Šemrov D, Mekid H, Mir LM. A validated model of in vivo electric field distribution in tissues for electrochemotherapy and for DNA electrotransfer for gene therapy. Biochim Biophys Acta 2000;1523:73–83.
11. Miyazaki S, Taniguchi H, Hachiya H, et al. Quantitative analysis of the isolation area during the chronic phase after a 28-mm second-generation cryoballoon ablation demarcated by high-resolution electroanatomic mapping. Circ Arrhythm Electrophysiol 2016;9:e003879.
12. Oakes RS, Badger TJ, Kholmovski EG, et al. Detection and quantification of left atrial structural remodeling with delayed-enhancement magnetic resonance imaging in patients with atrial fibrillation. Circulation 2009;119:1758–1767.
13. Rodríguez-Mañero M, Valderrábano M, Baluja A, et al. Validating left atrial low voltage areas during atrial fibrillation and atrial flutter using multielectrode automated electroanatomic mapping. JACC Clin Electrophysiol 2018; 4:1541–1552.
14. Anter E, Tschabrunn CM, Josephson ME. High-resolution mapping of scar-related atrial arrhythmias using smaller electrodes with closer interelectrode spacing. Circ Arrhythmia Electrophysiol 2015;8:537–545.
15. Kiuchi K, Kircher S, Watanabe N, et al. Quantitative analysis of isolation area and rhythm outcome in patients with paroxysmal atrial fibrillation after circumferential pulmonary vein antrum isolation using the pace-and-ablate technique. Circ Arrhythm Electrophysiol 2012;5:667–675.
16. Neumann E, Schaefer-Ridder M, Wang Y, Hofschneider PH. Gene transfer into mouse lyoma cells by electroporation in high electric fields. EMBO J 1982; 1:841–845.
17. Gehl J. Electroporation: theory and methods, perspectives for drug delivery, gene therapy and research. Acta Physiol Scand 2003;177:437–447.
18. Nanbu T, Yotsukura A, Suzuki G, et al. Important factors in left atrial posterior wall isolation using 28-mm cryoballoon ablation for persistent atrial fibrillation—block line or isolation area? J Cardiovasc Electrophysiol 2020; 31:119–127.
19. Kenigsberg DN, Martin N, Lim HW, Kowalski M, Ellenbogen KA. Quantification of the cryoablation zone demarcated by pre- and postprocedural electroanatomic mapping in patients with atrial fibrillation using the 28-mm second-generation cryoballoon. Heart Rhythm 2015;12:283–290.
20. Reddy VY, Neuzil P, d'Avila A, et al. Balloon catheter ablation to treat paroxysmal atrial fibrillation: what is the level of pulmonary venous isolation? Heart Rhythm 2008;5:353–360.
21. Nagashima K, Okumura Y, Watanabe I, et al. Hot balloon versus cryoballoon ablation for atrial fibrillation: lesion characteristics and middle-term outcomes. Circ Arrhythm Electrophysiol 2018;11:e005861.
22. Kapa S, Desjardins B, Callans DJ, Marchlinski FE, Dixit S. Contact electroanatomic mapping derived voltage criteria for characterizing left atrial scar in patients undergoing ablation for atrial fibrillation. J Cardiovasc Electrophysiol 2014; 25:1044–1052.
23. Squara F, Frankel DS, Schaller R, et al. Voltage mapping for delineating inexcitable dense scar in patients undergoing atrial fibrillation ablation: a new end point for enhancing pulmonary vein isolation. Heart Rhythm 2014; 11:1904–1911.